Optimization of Ring Stiffened Cylindrical Shells

Allen J. Bronowicki,* Richard B. Nelson,† Lewis P. Felton,‡ and Lucien A. Schmit Jr.§
University of California, Los Angeles, Calif.

This paper deals with the optimum structural design of circular cylindrical shells reinforced with identical uniformly spaced T-ring stiffeners, and subjected to external pressure loading. The optimization problems considered are of three types: 1) minimum-weight design, 2) design for maximum separation of the lowest two natural frequencies, and 3) design for maximum separation of the lowest two natural frequencies which have primarily axial content. Gross buckling is precluded by specifying a minimum natural frequency, and additional behavioral constraints preclude yielding or buckling of panels, T-ring stiffeners, and web and flange instabilities within each T-ring. The analysis is based on use of an equivalent orthotropic shell model, and optimization is accomplished through use of a sequential unconstrained minimization technique. Examples indicate that moderate increases in weight above optimum (minimum) values can result in more than a doubling of the frequency separations, and that maximum frequency separations are obtained when second and third lowest frequencies approach each other.

Nomenclature

$\{A\}_i$ = eigenvector of ith natural frequency
d_f = width of frame flange, in.
d_ϕ = depth of frame web, in.
E = Young's modulus
F = objective function
g = design constraint
$[K]$ = stiffness matrix
$[K_G]$ = geometric stiffness matrix
L = total length of structure, in.
ℓ = unsupported length of shell plating, in.
ℓ_x = spacing of frames, in.
$[M]$ = mass matrix
n,m = wave numbers
P = hydrostatic pressure, psi
P_{cr} = critical pressure for buckling of skin between frames, psi
q = number of design variables
R = radius to midsurface of skin, in.
r = positive scalar quantity
T = kinetic energy
t_f = thickness of frame flange, in.
t_s = thickness of shell skin, in.
t_ϕ = thickness of frame web, in.
u,v,w = midsurface displacements
$\bar{u},\bar{v},\bar{w}$ = displacements of an arbitrary point
W = normalized mass of structure
W_{max} = maximum allowable normalized structural mass
x,ϕ,z = shell coordinate system
ϵ = constant for use in computing extended penalty function
ν = Poisson's ratio
ϕ = composite objective function
ρ_s = mass density of structural material, slug/in.^{3}
σ_y = yield stress, psi
$\sigma_{f_{cr}}$ = critical flange buckling stress, psi
$\sigma_{w_{cr}}$ = critical web buckling stress, psi
τ = time, sec
ω = natural frequency
ω_{min} = minimum allowable natural frequency of vibration in vacuo, Hz

Received July 11, 1974; revision received May 12, 1975. This research was supported by the Office of Naval Research under Contract No. N00014-69-A0200-4048.

Index categories: Structural Design, Optimal; Structural Dynamic Analysis.

*Graduate student; currently with J. H. Wiggins Co., Redondo Beach, Calif.

†Associate Professor, Mechanics and Structures Department. Member AIAA.

‡Associate Professor, Mechanics and Structures Department. Associate Fellow AIAA.

§Professor, Mechanics and Structures Department. Associate Fellow AIAA.

I. Introduction

A WEALTH of literature has been devoted to the static, dynamic, and stability analyses of stiffened cylindrical shells of revolution subjected to various applied loads. The optimization of such structures has received much less attention since its introduction by Morrow and Schmit[1] in 1968. In this reference a cylindrical shell, reinforced with longitudinal and ring stiffeners, each with rectangular cross section, was designed to carry a number of independently applied sets of static loads with minimum structural weight. The shell was constrained against overall (system) buckling, panel and stiffener buckling, and also against material yield. The mathematical model which formed the basis for the stress and buckling analyses was an equivalent homogeneous orthotropic shell; i.e., the discrete stiffeners and skin stiffness properties were incorporated in the orthotropic elastic shell stiffness properties. This theory, a third-order Flugge-Lur'e-Byrne-type theory, proved adequate, provided that the stiffener spacing and cross-sectional dimensions were sufficiently small to permit the smoothing operation inherent in the orthotropic shell model.

In a more recent study, Pappas and Allentuch[2-5] investigated the minimum-weight design of ring stiffened cylindrical shells, subjected to a number of static applied load conditions. Here, the ring stiffeners were T-shaped rather than rectangular. In Refs. 2-4 the structural analyses of general instability, localized panel instability, and stiffener instabilities were based on buckling formulas contained in Ref. 6, along with appropriate stress limits. In Ref. 5 the analysis of general instability is based on the orthotropic shell model used in Ref. 7. Also, Pappas and Amba-Rao[8] have considered optimization of a stiffened cylinder with a minimum natural frequency constraint replacing the general instability constraint.

This paper presents a structural optimization study in which a combined and extended version of the structural models in Refs. 1-5 is employed to examine three distinct structural optimization problems. In the first problem, the minimum-weight design of a ring-stiffened cylindrical shell subjected to

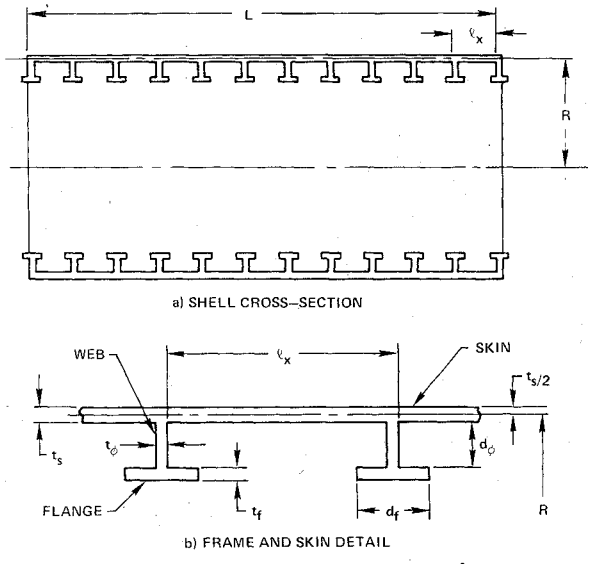

Fig. 1 Typical hull segment cross section.[2]

several applied static loads is considered. The structure is constrained against all of the local buckling modes considered in Refs. 2-5 although for some of the modes the constraint equations differ slightly. Further, as in Ref. 7, the structure is constrained against in vacuo natural vibrations below a specified frequency limit, a constraint which also accounts for gross buckling effects. In the second formulation the shell is designed to maximize the separation between the lowest two in vacuo natural frequencies, while being constrained against buckling and yield behavior as specified in the first design problem, and while having a weight less than a prescribed maximum. The third formulation is similar to the second, with the distinction that the frequencies being separated are the two lowest which have primarily axial content.

II. Analytical Formulation

Consider the optimum structural design of a circular cylindrical shell with uniformly spaced T-ring stiffeners (Fig. 1) and subjected to multiple applied loading conditions typical of submerged vessels, namely specified external pressure (or vessel depth), and specified axial compressive loadings. Design variables, shown in Fig. 1, are skin thickness t_s, stiffener web thickness t_ϕ, web depth d_ϕ, spacing ℓ_x, flange width d_f, and flange thickness t_f. Radius R, length L, and the material properties are assumed to be preassigned parameters. To investigate this structure the type of orthotropic shell model given in Ref. 1 is employed for the calculation of the natural frequencies of vibration and, hence, for the overall (system) buckling analysis. This idealization offers the advantage of mathematical simplicity, together with the minor disadvantage of somewhat limited modeling capability.¶

In order to analyze the dynamic response of the cylinder in Fig. 1, it is hypothesized (as in Ref. 1) that the frames and skin act as a unit according to the Bernoulli-Euler deformation assumption as extended through the Flugge-Lur'e-Byrne theory, and that the stiffness and inertia properties of the frames are uniformly distributed over the length of the cylinder. It is then possible to express the kinetic energy of the shell in the form

$$T=\frac{\rho_s}{2}\int_0^L\int_0^{2\pi}\int_t(\dot{\bar{u}}^2+\dot{\bar{v}}^2+\dot{\bar{w}}^2)\,dz\,d\phi\,dx \tag{1}$$

¶The model gives a very accurate representation of the structural behavior provided the characteristic wavelengths of the modes of vibration (or of the static displacements) are large compared to both the ring spacing and ring cross-sectional dimensions. Computational validity of the model was verified by comparison with exact solutions for discretely stiffened cylinders presented in Ref. 9. Under the conditions above, natural frequencies were found to agree within 5%.

where $\bar{u}$, $\bar{v}$, and $\bar{w}$ are the displacements of an arbitrary point in the structure in the x,ϕ, and z directions, respectively (Fig. 2), and are given by Ref. 1

$$\bar{u}=u-z\partial w/\partial x \tag{2a}$$

$$\bar{v}=(1-z/R)v-(z/R)\ (\partial w/\partial\phi) \tag{2b}$$

$$\bar{w}=w \tag{2c}$$

where u,v, and w are the displacements of the shell midsurface. From the kinetic energy the inertia terms in the appropriate equations of motion are obtained by use of Hamilton's principle. These terms are appended to the equations of static equilibrium for the stiffened shell in Ref. 1, which also contain the influence of destabilizing forces.

Assuming that the external loads give rise to circumferential and longitudinal compressive forces per unit length of magnitude PR and $PR/2$, respectively, where P is hydrostatic pressure, then the combination of inertia, static, and destabilizing forces leads to the following three coupled partial differential equations of motion

$$N_x'+\frac{1}{R}N_{\phi x}^*-\frac{P}{R}(u^{**}-Rw')-\frac{PR}{2}u''=p_x \tag{3a}$$

$$\frac{1}{R}N_\phi^*+N_{x\phi}'-\frac{1}{R}M_{x\phi}'-\frac{1}{R^2}M_\phi^*-\frac{P}{R}(v^{**}+w^*)-\frac{PR}{2}v''=p_y \tag{3b}$$

$$M_x''+\frac{1}{R}M_\phi^{*\prime}+\frac{1}{R}M_{x\phi}^{*\prime}+\frac{1}{R^2}M_{\phi x}^{*\prime}+\frac{1}{R}N_\phi+\frac{P}{R}(v^*-w^{**}-Ru'-\frac{R^2}{2}w'')=p_z \tag{3c}$$

where

$$p_x=\rho_s\int_t[\ddot{u}-z\ddot{w}'](1-\frac{z}{R})\,dz \tag{4a}$$

$$p_y=\rho_s\int_t[(1-\frac{z}{R})^2\ddot{v}-(1-\frac{z}{R})(\frac{z}{R})\ddot{w}^*](1-\frac{z}{R})\,dz \tag{4b}$$

$$p_z=\rho_s\int_t[\ddot{w}+z\ddot{u}'+(1-\frac{z}{R})(\frac{z}{R})\ddot{v}^*-(z)^2\ddot{w}''-(\frac{z}{R})^2\ddot{w}^{**}](1-\frac{z}{R})\,dz \tag{4c}$$

and where $\dot{(\ )}$ denotes $\partial(\ )/\partial\tau$, $(\ )'$ denotes $\partial(\ )/\partial x$, $(\ )^*$ denotes $\partial(\ )/\partial\phi$ and $\int_t(\ )dz$ is the integral through the thickness of the shell and frame. The forces M and N may be expressed in terms of the midsurface displacements u,v, and w (see Appendix A) so that Eqs. (3) can be expressed in terms of displacements only.

Under the assumption that the boundary conditions are of the simple support type, then the solution to these equations takes the form

$$u=A_1\sin n\phi\cos(m\pi x/L)\sin\omega t \tag{5a}$$

$$v=A_2\cos n\phi\sin(m\pi x/L)\sin\omega t \tag{5b}$$

$$w=A_3\sin n\phi\sin(m\pi x/L)\sin\omega t \tag{5c}$$

where $n=0,1,2,\ldots$ and $m=1,2,\ldots$

Substitution of Eqs. (5) into Eqs. (3) gives the algebraic

eigenvalue problem

$$([K]-P[K_G]-\omega^2[M])\{A\}=\{0\} \tag{6}$$

where the stiffness, "geometric" stiffness, and mass matrices are $[K]$, $[K_G]$, and $[M]$, respectively, and are given in Appendix A.

It should be noted that the sine and cosine dependencies on the angle ϕ, and the similar dependencies on the axial variable x can be interchanged without influencing the matrices in Eq. (6) for $n>0$. The $n=0$ case as given in Eq. (6) is actually a combination of the solution form in Eqs. (5) (pure torsion) and the similar form with sine and cosine terms (with argument zero) interchanged (torsionless motion).

Since the algebraic eigenvalue problem for given values of m, n, and P is of only rank three, its solution for the natural frequencies (eigenvalues) and associated modes (eigenvectors) may be easily obtained. In the structural optimization problem wherein the structure was designed for the greatest separation of the lowest two axial-type vibratory modes, the modes with $A_1=1$, and A_2, $A_3<1$ were termed "axial."

To prevent any general system buckling from occurring, all the frequencies associated with values $n=0,\ldots,6$, $m=1,\ldots,6$ were retained and forced to exceed a prescribed minimum, $\omega_{\min}$. Although these values of m and n may not always encompass the lowest vibratory modes, they provide a practical upper limit for the structural model considered herein, i.e., higher values of m and n would correspond to modes for which the orthotropic shell model is incapable of providing an accurate representation of the discretely stiffened shell.

In addition to gross buckling, it is necessary to be able to detect the occurrence of several additional modes of "local" failure. These local failure modes consist of panel (interring) yielding or buckling and yielding or buckling of the webs and/or flanges of the stiffener rings. It may be noted that local buckling could also be precluded by requiring appropriate vibratory modes to have frequencies greater than zero. However, inclusion of a sufficient number of mode shapes to accommodate such an analysis would be beyond the scope of this paper and would, again, be inconsistent with the use of the orthotropic shell model. Consequently, local failure analyses are based on static criteria, as detailed in the following.

Panel (skin) yielding will not occur, according to the Von Mises criterion, provided

$$(\sigma_\phi^2-\sigma_\phi\sigma_x+\sigma_x^2)^{1/2}\le\sigma_y \tag{7}$$

where σ_y = material yield stress in uniaxial loading, and σ_ϕ and σ_x are inplane stresses normal to the surfaces of the element in Fig. 2. From Ref. 6 the maximum bending stresses in the panels due to external pressure are

$$\sigma_\phi=-(PR/t_s)[1+\Gamma(H_n+\nu H_E)] \tag{8a}$$

$$\sigma_x=-(PR/t_s)(\tfrac{1}{2}+\Gamma H_E) \tag{8b}$$

where Γ, H_E, and H_n are load factors defined in Appendix B.

A suitable approximate formula[6] for the critical external pressure which will cause panel buckling is

$$P_{cr}=2.42E(t_s/D)^{5/2}/\{(1-\nu^2)^{3/4}[(\ell/D)-0.45(t_s/D)^{1/2}]\} \tag{9}$$

where $\ell=\ell_x-t_\phi$ is the unsupported length of a panel, and $D=2R$.

Again following Ref. 6, the maximum compressive stress in the rings may be taken as

$$\sigma_c=-PRQ/A \tag{10}$$

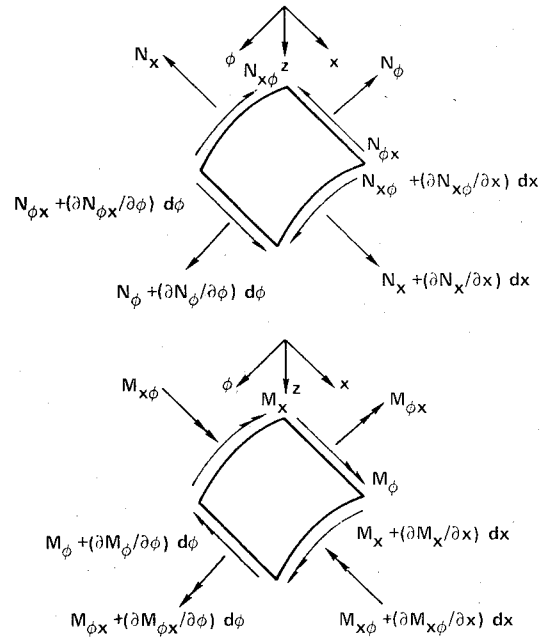

Fig. 2 Force resultants and coordinate system.

where $A=t_st_\phi+t_\phi d_\phi+t_fd_f$, and Q is a load factor defined in Appendix B. The magnitude of σ_c must be less than the yield stress σ_y, and also less than the critical values of compressive stresses at which the flange or web will buckle. Assuming that the web and flange are very long rectangular plates, that the web is simply supported along all edges, and that the flange is simply supported along three sides and free on one edge (all conservative assumptions), then the critical stresses for buckling of the flange and web, respectively, are[10]

$$\sigma_{f_{cr}}=[0.506\pi^2E/12(1-\nu^2)]\,[2t_f/(d_f-t_\phi)]^2 \tag{11a}$$

$$\sigma_{w_{cr}}=[4\pi^2E/12(1-\nu^2)]\,[t_\phi/d_\phi]^2 \tag{11b}$$

It should be noted that Eq. (10) neglects any effects of lateral-torsional stiffener buckling on the compressive stress in the rings, and also ignores eccentricity in the geometry of the cylinder, although this latter effect may be significant.[8]

III. Formulation of Optimization Problem

As indicated in Sec. I, the optimization problems considered herein take the following three alternative forms:

1) Find the minimum-weight design of the stiffened cylindrical shell subjected to the predetermined applied loads and constrained against panel (inter-ring) buckling, T-web and/or flange buckling, panel and/or ring yield. The shell is also required to possess a lowest natural frequency (in vacuo) greater than a specified minimum.

2) Find the structural design which maximizes the separation between the lowest two natural frequencies of vibration (in vacuo) for the stiffened cylindrical shell subjected to the predetermined applied loads and constrained against panel (interring) buckling, T-web and/or flange buckling, panel and/or ring yield. The shell is also required to possess a lowest natural frequency greater than a specified minimum, and a structural weight less than a prescribed maximum.

3) Find the structural design which maximizes the separation between the lowest two natural frequencies of vibration (in vacuo) which have primarily axial content for the stiffened cylindrical shell subjected to the predetermined applied loads and constrained against panel (interring) buckling, T-web and/or flange buckling, panel and/or ring yield. The shell is also required to possess a lowest natural frequency

greater than a specified minimum and a structural weight less than a prescribed maximum.

Each of these problems is an inequality-constrained optimization problem, which may be solved by any of a number of mathematical programing algorithms. The particular method of solution chosen for this work is the Sequential Unconstrained Minimization Technique (SUMT) in which the inequality-constrained problem (in form 1, 2, or 3) is converted into a sequence of unconstrained problems[11] by means of so-called "penalty functions." In this technique, it is required to find a vector $X^T = \{x_1 x_2 \ldots x_i \ldots x_q\} \equiv \{t_s t_\phi d_\phi \ell_x d_f t_f\}$, the components of which are the design variables, such that a specified function of these variables, $F(X)$, is extremized while satisfying a set of constraints of form $g_k(X) \geq 0$, $k = 1,\ldots,s$. This algorithm produces a sequence of designs which approach a local (or possibly global) optimum from the feasible portion of the design space, and each of which is unconstrained, i.e., has no critical constraints. This is a desirable feature from the standpoint of producing "safe" designs, but also one which gives slightly less optimal results than other algorithms which give a sequence of ctitically constrained designs.

The objective function, $F(X)$, takes one of three forms, depending on the optimization problem being considered. For problem 1, weight minimization,

$$F(X) = W = \frac{2\pi\rho_s}{\pi(R+t_s/2)^2 L\rho_w}\{RLt_s + (L/\ell_x)[(R-e_\phi)t_\phi d_\phi + (R-e_f)t_f d_f]\} \tag{12}$$

where parameters e_ϕ and e_f are defined in Appendix A. In Eq. (12) $F(X)$ has been normalized by dividing shell mass by the mass of displaced water (ρ_w = mass density of water).

For problem 2, the case of separation of lowest natural frequencies, an inverse formulation is used. The separation is maximized by minimizing the inverse of the separation. For the modes being considered, an ordered list is made giving $\omega_1 < \omega_2 < \omega_3$, etc. The objective function is then

$$F(X) = \Delta_1/(\omega_2 - \omega_1) \tag{13}$$

where Δ_1 is a normalization factor taken as the initial frequency separation. To separate frequencies having primarily a longitudinal deformation content, (problem 3), it is necessary to examine and order frequencies in each "primarily axial" mode, i.e., the ones having both A_2 and A_3 smaller than A_1. The objective function is then given by

$$F(X) = \Delta_1/(\omega_{L_2} - \omega_{L_1}) \tag{14}$$

where the subscript L has been added to denote the longitudinal character of the shell vibration,

The number of design variables q is a maximum of six in this study, but may be less if certain of the design variables are fixed or linked. Also, upper and lower limits U_i and L_i, respectively, are assumed specified for each variable x_i. These upper and lower limit constraints, respectively, are written in the normalized form

$$g_i(X) = (U_i - x_i)/(U_i - L_i) \geq 0 \tag{15}$$

$$g_{q+i}(X) = (x_i - L_i)/(U_i - L_i) \geq 0 \tag{16}$$

where $i = 1,\ldots q$. It is also necessary to include a geometric admissability constraint, which serves to keep the frame flanges from overlapping. This is expressed in the normalized form

$$g_{2q+1}(X) = 1 - d_f/\ell_x \geq 0 \tag{17}$$

The behavioral constraints may also be normalized. The panel yield constraint is expressed as

$$g_{2q+2}(X) = 1 - (\sigma_\phi^2 - \sigma_x\sigma_\phi + \sigma_x^2)^{1/2}/\sigma_y \geq 0 \tag{18}$$

and the frame yield, flange buckling, web buckling, and skin buckling constraints, respectively, are written as

$$g_{2q+3}(X) = 1 - |\sigma_c|/\sigma_y \geq 0 \tag{19}$$

$$g_{2q+4}(X) = 1 - |\sigma_c|/\sigma_{f_{cr}} \geq 0 \tag{20}$$

$$g_{2q+5}(X) = 1 - |\sigma_c|/\sigma_{w_{cr}} \geq 0 \tag{21}$$

$$g_{2q+6}(X) = 1 - P/P_{cr} \geq 0 \tag{22}$$

Finally, to prevent gross buckling the lowest frequency ω_1 is required to be greater than a specified minimum frequency $\omega_{\min}$. This is stated in the form

$$g_{2q+7}(X) = (\omega_1 - \omega_{\min})/\Delta_2 \geq 0 \tag{23}$$

where Δ_2 is the initial value of $\omega_1 - \omega_{\min}$.

For the minimum-weight design of the shell these are all the constraints required, but in order to separate frequencies, two other constraints must be included. It is conceivable that large separations could be achieved, but possibly only at the expense of large increases in weight. It is, therefore, necessary to establish an upper bound to the mass of the structure $W_{\max}$. The constraint is expressed by

$$g_{2q+8}(X) = 1 - W/W_{\max} \geq 0 \tag{24}$$

A final constraint, which is not actually required in the definition of the frequency separation problem, is convenient to include for the numerical solution when penalty functions are utilized in the Sequential Unconstrained Minimization Technique. The most efficient unconstrained minimization methods require the computation of gradients of the objective function in order to operate. These gradients should be smooth and continuous, but experience shows that, as ω_1 and ω_2 are separated, ω_2 and ω_3 approach a common value. Eventually, ω_2 and ω_3 will cross, with the result that the mode which previously represented ω_2 now represents ω_3 and vice versa. This causes a discontinuity in the gradient of the objective function and subsequent difficulties with the numerical algorithm. This difficulty may be simply overcome by requiring that the second and third frequencies never be equal. This "singularity avoidance" constraint in the two cases of frequency separation then becomes

$$g_{2q+9}(X) = \omega_3 - \omega_2 > 0 \tag{25}$$

or

$$g_{2q+9}(X) = \omega_{L_3} - \omega_{L_2} > 0 \tag{26}$$

To apply the SUMT method, the basic inequality-constrained problem is recast in the form of an interior penalty function,[11] the solution of which requires finding the design vector X which minimizes

$$\Phi(X) = F(X) + r\sum_{J=1}^{s} P_j(X) \tag{27a}$$

where

$$P_j(X) = \begin{cases} 1/g_j(X) & \text{if } g_j(X) \geq \epsilon \\ [2\epsilon - g_j(X)]/\epsilon^2 & \text{if } g_j(X) < \epsilon \end{cases} \tag{27b}$$

$P_j(X)$ is the so-called extended penalty function,[12] which allows the use of infeasible designs in the search for an optimal feasible solution. The quantities ϵ and r are small positive scalars and s is the total number of constraints. Solving this unconstrained minimization problem for suc-

cessively smaller values of r gives a series of designs which converge to a local or global optimum of $F(X)$. In this study, each unconstrained minimization was performed by the Davidon-Fletcher-Powell method.[11] To apply this algorithm it is necessary to compute the gradients of the objective function and the constraints. The mathematical complexity associated with analytic calculation of partial derivatives makes it convenient to use a forward difference technique to find the gradients numerically. Finally, since the success of the unconstrained minimization depends heavily on the determination of an accurate unidirectional minimum, a special hyperbolic interpolation formula was developed[11] for use with the SUMT method.

IV. Examples

Design examples given in Ref. 3 were re-evaluated in this study for optimal performance for situations 1, 2, or 3, as previously detailed. In all of these designs the preassigned parameters were given the following values: $R=198$ in., $L=594$ in., $E=30\times10^6$ psi, $\sigma_y=60\times10^3$ psi, $\rho_s=7.75\times10^{-4}$ slug/in.^{3}, $\nu=0.33$, and specified pressure associated with depths in water of 1000, 2000, and 3000 ft, where $\rho_w=0.959\times10^{-4}$ slug/in.^{3}. The prescribed minimum natural (in vacuo) frequency was taken as 12.0 Hz. Except for the dynamic effects, these problems are quite similar to those examined in Ref. 3. The structures was designed initially for minimum weight (problem 1) for the three different operating depths. The results given in Table 1 indicate normalized minimum weights of 0.11274, 0.21272, and 0.31373 for operating depths of 1000, 2000, and 3000 ft, respectively,** values slightly different from those reported in Ref. 3 [3].†† This is due to the fact that the web and flange thicknesses were included herein as independent design variables, while in Ref. 3 the web and flange thicknesses were linked together. Also, system buckling effects are treated by a dynamic analysis in this study, and in Ref. 3 by a static stability analysis modified by use of safety factors. The designs presented in Table 1 are actively constrained by skin yielding, web buckling, and flange buckling. The design for 1000-ft depth is also constrained by minimum frequency.

One important benefit in obtaining the minimum-weight designs is that they serve as initial, feasible designs for problems 2 and 3, provided the same minimum frequency constraint is employed and the maximum allowable structural mass is greater than that of the minimum-weight design for the static load conditions. However, these designs are sensitive to the choice of starting points. In particular, the use of local minimum-weight designs reported in Ref. 13 as starting points for problems 2 and 3 led to better results than did the use of values in Table 1.

The results of design problem 2, optimization for maximum frequency separation, are given in Table 2 for the same three preassigned operating depths. The maximum allowable normalized weights were taken from 10% to 30% greater than those for the minimum-weight designs for the static load condition, the values being 0.15, 0.25, and 0.35, respectively, for the operating depths of 1000, 2000, and 3000 ft. For the three depth requirements the frequency separation was increased from the minimum-weight design values of 10.87, 9.25, and 4.55 Hz to 23.59, 24.28, and 25.33 Hz. Of interest is the fact that the first and third solutions (for 1000-ft and 3000-ft operating depths) gave frequencies $\omega_2=\omega_3$, i.e., nearly identical second and third frequencies and that in these two cases the maximum-weight constraint was less than critical. It is thus apparent that the major portion of the frequency separation is obtained by bringing the second frequency up to the third frequency, and that little or nothing is to be gained by adding more material to the structure after this is accomplished. In the example with 2000-ft depth, the second and third frequencies were unable to approach each other completely before violating the maximum-weight constraint, which became critical in this case. It may be noted that for these designs the frame webs are very thin and the frame flanges are relatively thick. It thus seems that the frequency separation has been achieved by making the moment of inertia of the frames as large as possible.

Three problems of category 3 were designed to find the maximum frequency separation in primarily longitudinal

Table 1 Design problem 1—weight minimization

Depth	1000 ft	2000 ft	3000 ft
t_s, in.	1.2056	2.4012	3.6132
t_ϕ, in.	0.2373	0.3136	0.3881
d_ϕ, in.	11.020	14.046	16.697
ℓ_x, in.	30.170	32.904	36.221
d_f, in.	10.363	11.168	12.969
t_f, in.	0.3071	0.3409	0.3975
ω_1, Hz	12.03	14.33	19.74
ω_2, Hz	22.90	23.58	24.29
ω_3, Hz	30.30	44.63	42.85
Weight (normalized)	0.11274	0.21272	0.31373

Table 2 Design problem 2—frequency separation

Depth	1000 ft	2000 ft	3000 ft
t_s, in.	1.2216	2.4717	3.3986
t_ϕ, in.	0.3950	0.3884	0.5168
d_ϕ, in.	20.722	19.674	23.764
ℓ_x, in.	33.853	51.417	36.065
d_f, in.	17.551	15.075	16.864
t_f, in.	0.4653	1.8638	0.9485
ω_1, Hz	28.3711	29.4905	29.7225
ω_2, Hz	51.9638	53.7674	55.0508
ω_3, Hz	51.9640	54.1466	55.0512
Weight[a] (normalized)	0.1351	0.25	0.32928
$(\omega_2-\omega_1)$ Hz	23.5928	24.2769	25.3283

[a]Maximum (upper bound) weights (normalized) are 0.15, 0.25, and 0.35, respectively.

Table 3 Design problem 3—longitudinal frequency separation

Depth	1000 ft	2000 ft	3000 ft
t_s, in.	1.5975	2.6720	3.9377
t_ϕ, in.	0.2500	0.4171	0.42116
d_ϕ, in.	11.603	17.384	19.817
ℓ_x, in.	38.672	52.232	36.143
d_f, in.	9.1454	13.232	16.907
t_f, in.	0.3826	0.5248	0.4927
ω_{L_1}, Hz	163.0006	163.0640	138.2134
ω_{L_2}, Hz	192.2375	192.7389	162.4559
ω_{L_3}, Hz	222.6656	222.7126	221.6170
Weight[a] (normalized)	0.14215	0.23559	0.34907
$(\omega_{L_2}-\omega_{L_1})$, Hz	29.2369	29.6749	24.2425

[a]Maximum (upper bound) weights (normalized) are 0.15, 0.25, and 0.35, respectively.

**Results in Table 1 differ from corresponding results reported in Ref. 13. Results for the 1000- and 2000-ft cases in Ref. 13 are evidently local minimums, and improved designs have subsequently been obtained. Also, more complete convergence to a minimum design has been obtained for the 3000-ft case. The authors wish to thank M. Pappas for bringing the existence of improved designs to their attention.

††Results in Ref. 3 are based on $\rho_s=7.30\times10^{-4}$ slug/in.^{3}, and $\nu=0.30$, rather than the values used herein. The objective function in Ref. 3 is also slightly different, with an integer k (the number of rings in the shell) replacing the factor L/ℓ_x in Eq. (12).

modes of vibration for the three different operating depths. Results are given in Table 3. For the cases which have operating depths of 1000 ft and 2000 ft the algorithm became entrapped in a singularity in the design space. The problem run at 3000-ft depth was unable to reach the singularity because the maximum weight constraint had become active. A singularity avoidance constraint could have been developed to enable the algorithm to proceed, however, this was not done because the primary reason for this problem was contained in the basic definition of "axial" modal content. For the 3000-ft case, the mode $m=1$, $n=0$ has a "longitudinal" frequency of 138.21 Hz (Table 3), because the v-component of the associated eigenvector is zero and the w-component is less than 1.0 (0.977). As the algorithm separates the frequencies, the eigenvector associated with this frequency changes form, with the w-component increasing to a value slightly greater than 1.0. As this occurs, a second eigenvector of this mode's vibratory class ($m=1$, $n=0$) becomes longitudinal in form, according to the definition in the design problem statement. The result is the situation encountered for the 1000-ft and 2000-ft cases, where the $m=1$, $n=0$ mode has the second lowest frequency. The algorithm becomes entrapped at a point in the design space at a frequency separation of 29 Hz as two eigenvectors for the $m=1$, $n=0$ mode switch back and forth, having w-components both approximately equal to 1.0, i.e., the $m=1$, $n=0$ mode has two frequencies of vibration with identical axial content.

V. Conclusions

The designs obtained in this study indicate both the utility and benefit that automated design procedures bring to the design process. Although based on a simplified structural model, these designs satisfy many of the behavioral characteristics which must be accounted for in practical design situations. Consequently, it is anticipated that this type of optimization, when based on a more sophisticated model, will provde an important step in bridging the gap that currently exists between automated design and design practice.

Appendix A: Dynamic Analysis

The forces on the cylindrical shell (see Fig. 2) are expressed in terms of displacements as

$$N_x = Hu' + (H\nu/R)v^* - (H\nu/R)w + (D/R)w''$$

$$N_\phi = H\nu u' + [(H+HC+HF)/R]v^* - [H+HC(1+e_\phi/R)+HF(1+e_f/R)]w/R - [D/R+HC(e_\phi+\rho_\phi^2/R)+HF(e_f+\rho_f^2/R)]\frac{1}{R^2}w^{**}$$

$$N_{x\phi} = (S/R)u^* + Sv' + (K/R^2)w'^*$$

$$N_{\phi x} = (S/R)u^* + Sv' - (K/R^2)w'^*$$

$$M_x = -(D/R)u' - (D\nu/R^2)v^* - Dw'' - (D\nu/R^2)w^{**}$$

$$M_\phi = (HCe_\phi/R + HFe_f/R)v^* - [D/R+HC(e_\phi+\rho_\phi^2/R)+HF(e_f+\rho_f^2/R)]w/R - D\nu w'' - [D+HC(\rho_\phi^2+\alpha_\phi^3/R) + HF(\rho_f^2/R)]w^{**}/R^2$$

$$M_{x\phi} = -(2K/R)(v'+w'^*)$$

$$M_{\phi x} = (K/R^2)u^* - (K/R)v' - (2K+Q)w'^*/R$$

$$()^* = \partial()/\partial\phi \qquad ()' = \partial()/\partial x$$

The matrices $[K]$, $[K_G]$, and $[M]$ in Eq. (6) are

$$[K] = \begin{bmatrix} k_{11} & k_{12} & k_{13} \\ k_{12} & k_{22} & k_{23} \\ k_{13} & k_{23} & k_{33} \end{bmatrix}$$

$$k_{11} = -H\lambda^2 - (S/R^2)n^2$$

$$k_{12} = -(H\nu+S)\lambda n/R$$

$$k_{13} = -[H\nu\lambda + D\lambda^3 - (K/R^2)\lambda n^2]/R$$

$$k_{22} = -(S+2K/R^2)\lambda^2 - [H+HC(1-e_\phi/R) + HF(1-e_f/R)]n^2/R^2$$

$$k_{23} = -(3K+D\nu)\lambda^2 n/R^2 + [D/R^2 - H + HC(\rho_\phi^2/R^2 - 1) + HF(\rho_f^2/R^2 - 1)]n/R^2 - [HC(\alpha_\phi^3/R^2 - e_\phi) + HF(\alpha_f^3/R^2 - e_f)]n^3/R^3$$

$$k_{33} = -[H+HC(1+e_\phi/R)+HF(1+e_f/R)]/R^2 + 2[D/R+HC(e_\phi+\rho_\phi^2/R)+HF(e_f+\rho_f^2/R)]n^2/R^3 - D\lambda^4 - [2D\nu+4K+Q](\lambda n/R)^2 - [D+HC(\rho_\phi^2+\alpha_\phi^3/R)+HF(\rho_f^2+\alpha_f^3/R)](n/R)^4$$

$$[K_G] = \begin{bmatrix} k_{G_{11}} & 0 & k_{G_{13}} \\ 0 & k_{G_{22}} & k_{G_{23}} \\ k_{G_{13}} & k_{G_{23}} & k_{G_{33}} \end{bmatrix}$$

$$k_{G_{11}} = -(n^2+\lambda^2/2)/R \qquad k_{G_{23}} = n/R$$

$$k_{G_{13}} = -\lambda \qquad k_{G_{33}} = -(n^2+\lambda^2/2)/R$$

$$k_{G_{22}} = -(n^2+\lambda^2/2)/R$$

$$M = \begin{bmatrix} m_{11} & 0 & m_{13} \\ 0 & m_{22} & m_{23} \\ m_{13} & m_{23} & m_{33} \end{bmatrix}$$

$$m_{11} = t_s + A(1-e_\phi/R) + B(1-e_f/R)$$

$$m_{13} = [t_s^3/(12R) + A(-e_\phi+\rho_\phi^2/R) + B(-e_f+\rho_f^2/R)]\lambda$$

$$m_{22} = t_s\left(1+\frac{t_s^2}{4R^2}\right) + A(1-3e_\phi/R+3\rho_\phi^2/R^2-\alpha_\phi^3/R^3) + B(1-3e_f/R+3\rho_f^2/R^2-\alpha_f^3/R^3)$$

$$m_{23} = [t_s^3/(6R^2) + A(-e_\phi/R+2\rho_\phi^2/R^2-\alpha_\phi^3/R^3) + B(-e_f/R+2\rho_f^2/R^2-\alpha_f^3/R^3)]n$$

$$m_{33} = t_s + (\lambda^2+n^2/R^2)t_s^3/12 + A[1-e_\phi/R + (\lambda^2+n^2/R^2)(\rho_\phi^2-\alpha_\phi^3/R)] + B[1-e_f/R+(\lambda^2+n^2/R^2)(\rho_f^2-\alpha_f^3/R)]$$

The section properties are defined as follows:

$$H = Et_s/(1-\nu^2) \qquad D = Et_s^3/[12(1-\nu^2)]$$

$$A = t_\phi d_\phi/\ell_x \qquad B = t_f d_f/\ell_x$$

$$HC = EA \qquad HF = EB$$

$$G = E/[2(1+\nu)] \qquad t_t = t_s + 2d_\phi$$

$$S = Gt_s \qquad K = Gt_s^3/12$$

$$Q = G(J_\phi + J_f)\ell_x$$

$$J_\phi = c_\phi d_\phi t_\phi^3$$

$$c_\phi = -0.285\, e^{-(0.49 d_\phi / t_\phi)} + 0.316$$

$$J_f = c_f d_f t_f^3$$

$$c_f = -0.285\, e^{-(0.49\, d_f/t_f)} + 0.316$$

$$e_\phi = \tfrac{1}{2}(d_\phi + t_s)$$

$$e_f = \tfrac{1}{2}(d_f + t_t)$$

$$\rho_\phi^2 = \tfrac{1}{3}d_\phi^2 + \tfrac{1}{2}d_\phi t_s + \tfrac{1}{4}t_s^2$$

$$\rho_f^2 = \tfrac{1}{3}d_f^3 + \tfrac{1}{2}d_f t_t + \tfrac{1}{4}t_t^2$$

$$\alpha_\phi^3 = \tfrac{1}{4}d_\phi^3 + \tfrac{1}{2}t_s d_\phi^2 + (3/8)t_s^2 d_\phi + \tfrac{1}{8}t_s^3$$

$$\alpha_f^3 = \tfrac{1}{4}d_f^3 + \tfrac{1}{2}t_t d_f^2 + (3/8)t_t^2 d_f + \tfrac{1}{8}t_t^3$$

Appendix B: Static Strength Analysis

The critical compressive stresses in the skin are assumed to occur on the outer surface at midpanel, where the stresses are

$$\sigma_\phi = -(PR/t_s)[1 + \Gamma(H_n + \nu H_E)]$$

$$\sigma_x = -(PR/t_s[\tfrac{1}{2} + \Gamma H_E]$$

with the various parameters defined as

$-PR/t_s$ = hoop stress

R = radius to midplane of shell

$\Gamma = [1 - \nu/2 - B]/(1+\beta)$

B = ratio of shell area under frame web to total frame area $= t_s t_\phi / A$

$A = t_s t_\phi + t_\phi d_\phi + t_f d_f$

$\beta = 2N\{1/[3(1-\nu^2)]\}^{1/4}(Rt_s^3)^{1/2}/A$

$N = (\cosh\theta - \cos\theta)/(\sinh\theta + \sin\theta)$

$\theta = \ell[3(1-\nu^2)/(Rt_s)^2]^{1/4}$

ℓ = unsupported length of shell $= \ell_x - t_\phi$

$$H_n = -2[\sinh(\theta/2)\cos(\theta/2) + \cosh(\theta/2)\sin(\theta/2)]/(\sinh\theta + \sin\theta)$$

$$H_E = -2[3/(1-\nu^2)]^{1/2}[\sinh(\theta/2)\cos(\theta/2) - \cosh(\theta/2)\sin(\theta/2)]/(\sinh\theta + \sin\theta)$$

The hoop compressive stress in the frame is

$$\sigma_c = PVR/A$$

where V is a load factor given as

$$V = t_\phi[1 + (1-\nu/2)\beta/B]/(1+\beta)$$

References

[1] Morrow, W. M. and Schmit, L. A., "Structural Synthesis of a Stiffened Cylinder," CR-1217, Dec. 1968, NASA.

[2] Pappas, M. and Allentuch, A., "Structural Synthesis of Frame Reinforced Submersible, Circular, Cylindrical Hulls," Rept. No. NV5, May 1972, Newark College of Engineering, Newark, N.J.

[3] Pappas, M. and Allentuch, A., "Optimal Design of Submersible Frame Stiffened, Circular Cylindrical Hulls," Rept. No. NV6 (Rev.), July 1972, Newark College of Engineering, Newark, N.J.

[4] Pappas, M. and Allentuch, A., "Structural Synthesis of Frame Reinforced, Submersible, Circular, Cylindrical Hulls," *Computers and Structures*, Vol. 4, March 1974, pp. 253-280.

[5] Pappas, M. and Allentuch, A., "Pressure Hull Optimization Using General Instability Equations Admitting More Than One Longitudinal Buckling Half-Wave," Rept. No. NV9, June 1973, Newark College of Engineering, Newark, N.J.

[6] *Principles of Naval Architecture*, Society of Naval Architects and Marine Engineers, New York, 1967.

[7] McElman, J. A., Mikulas, M. M., and Stein, M., "Static and Dynamic Effects of Eccentric Stiffening of Plates and Cylindrical Shells," *AIAA Journal*, Vol. 4, May 1966, pp. 887-894.

[8] Pappas, M. and Amba-Rao, C. L., "Direct Search Algorithm for Automated Optimum Structural Design," *AIAA Journal*, Vol. 9, March 1971, pp. 387-393.

[9] Forsberg, K., "Exact Solution for Natural Frequencies of Ring-Stiffened cylinders," *Proceedings of the AIAA/ASME 10th Structures, Structural Dynamics and Materials Conference*, New Orleans, La., April 1969.

[10] Timoshenko, S. P. and Gere, J. M., *Theory of Elastic Stability*, 2nd ed., McGraw-Hill, New York, 1961.

[11] Fox, R. L., *Optimization Methods for Engineering Design*, Addison-Wesley, Reading, Mass, 1971.

[12] Kavlie, D. and Moe, J., "Automated Design of Frame Structures," *ASCE Journal of the Structural Division*, Vol. 97, Jan. 1971, pp. 33-62.

[13] Bronowicki, A. J., Nelson, R. B., Felton, L. P., and Schmit, L. A., Jr., "Optimum Design of Ring Stiffened Cylindrical Shells," UCLA-ENG-7414, Feb. 1974, School of Engineering and Applied Science, UCLA, Los Angeles, Calif.